

TOP AND ELECTROWEEK RESULTS FROM THE TEVATRON

ANDREW IVANOV
(for the CDF and DØ Collaborations)

University of California, Davis, U. S. A.
E-mail address: andrew@fnal.gov

Received 5 November 2007; Accepted 27 February 2008
Online 18 June 2008

Recent results from CDF and DØ experiments on W and Z bosons and top quark properties are presented.

PACS numbers: 14.70.Fm, 14.70.Hp, 14.65.Ha

UDC 529.126

Keywords: DØ, Tevatron, W boson, Z boson, top quark

1. Introduction

Run 2 of the Fermilab Tevatron started proton-antiproton collisions at the center-of-mass energy $\sqrt{s} = 1.96$ TeV in 2001 after extensive upgrades of the accelerator complex and CDF and DØ detectors. The accelerator performance has been improving since the beginning of the Run 2. As of October 2007, the Tevatron has achieved record peak luminosity of $2.9 \times 10^{32} \text{ cm}^{-2}\text{s}^{-1}$, and is expected to supersede that next year. Approximately 50 pb^{-1} of integrated luminosity of data, half the size of the Tevatron Run1 dataset, is being accumulated weekly, and at the moment of writing, 2.7 fb^{-1} of integrated luminosity has been written on tape by each experiment. The current performance projections aim for $6-8 \text{ fb}^{-1}$ by the end of Run 2.

Results presented here use the data corresponding to the integrated luminosities ranging from 0.2 fb^{-1} to 1.7 fb^{-1} , collected by CDF and DØ in 2002–2006. Both detectors are similar in their capabilities of detecting W/Z bosons and top quarks. Each detector utilizes inner silicon precision tracking system with large-volume cylindrical tracker chambers immersed in a solenoidal magnetic field. The magnets are surrounded by the electromagnetic and hadronic calorimeters and further out by muon chambers. All of the components of the detectors are critical for the electroweak and top physics analyzes. A detailed description of upgraded detectors is given in Ref. [1].

2. Electroweak physics at the Tevatron

W and Z bosons are produced at the Tevatron through $q\bar{q}$ annihilation. The samples of leptonic decays of W and Z into electrons and muons have a clean experimental signature with a low background and comprise the most incisive event samples for Standard Model (SM) precision tests, such as measurements of W mass and width, and for probing the quantum-chromodynamic (QCD) aspects of the production mechanism that provides stringent constraints on the parton distribution functions (PDFs).

Inclusive W and Z production cross sections have been measured in all three lepton (e, μ, τ) channels [2] and have been found to be in agreement with the NNLO calculations [3]. The precision of the measurements is dominated by systematic uncertainties, primarily due to the uncertainty in the Tevatron luminosity of $\sim 6\%$ [4], and other systematic uncertainties due to PDFs, lepton identification efficiency and backgrounds of $\sim 2\%$.

2.1. W mass and width measurements

The W boson mass (M_W) is a fundamental parameter of the SM, which receives self-energy corrections Δr due to vacuum fluctuations involving virtual particles. In the SM, the contributions to Δr are dominated by the top quark and the Higgs boson loops, such that a precise measurement of M_W in conjunction with the top quark mass constrains the mass m_H of the Higgs boson.

The W mass is measured in the $e\nu$ and $\mu\nu$ channels using a sample of 200 pb^{-1} of the CDF data by performing a maximum-likelihood fit to the transverse lepton momentum (p_T^ℓ) distribution, the transverse neutrino momentum (p_T^ν) distribution, obtained from imposing p_T balance in the event, and the transverse mass, defined as $m_T = \sqrt{2p_T^\ell p_T^\nu (1 - \cos[\phi^\ell - \phi^\nu])}$.

The key ingredient of the measurement is the calibration of the lepton energy. The momentum scale is set by J/Ψ and $\Upsilon(1S)$ dimuon mass peaks, giving consistent results with the Z boson mass fit. The energy measurement in the electromagnetic (EM) calorimeter is calibrated from the fit to the peak of the E/p electron distribution in the $W \rightarrow e\nu$ sample. The radiative energy loss is tuned using the radiative tail of the E/p distribution. Hadronic recoil response and resolution parameterizations are obtained from the p_T -imbalance in $Z \rightarrow \ell\ell$ events as a function of boson p_T .

The combined result of the six W boson mass fits, including correlations, is $M_W = (80413 \pm 34 \text{ (stat)} \pm 34 \text{ (syst)}) \text{ MeV}/c^2$ [5], which is the most precise single measurement to date. Inclusion of this result increases the world average W boson mass to $M_W = (80398 \pm 25) \text{ MeV}/c^2$ [6], reducing the total uncertainty by 15%. The uncertainties of the measurement are shown in Table 1, where most of the systematic uncertainties are limited by the statistics of the control samples used. By the end of Run 2, the W boson mass is expected to be measured with a precision of $20\text{--}25 \text{ MeV}/c^2$, better than the current world average.

TABLE 1. The uncertainties on the CDF M_W and Γ_W measurements. The last column for each measurement shows the correlated uncertainties.

| Uncertainty | ΔM_W (MeV/c ²) | | | $\Delta \Gamma_W$ (MeV/c ²) | | |
|-----------------------|------------------------------------|-------|--------|---|-------|--------|
| | Electrons | Muons | Common | Electrons | Muons | Common |
| Lepton Energy Scale | 30 | 17 | 17 | 21 | 17 | 12 |
| Lepton En. Resolution | 9 | 3 | 0 | 31 | 26 | 0 |
| Simulation | - | - | - | 13 | 0 | 0 |
| Recoil | 12 | 12 | 12 | 54 | 49 | 0 |
| Lepton ID | 3 | 1 | 0 | 10 | 7 | 0 |
| Lepton Removal | 8 | 5 | 5 | - | - | - |
| Backgrounds | 8 | 9 | 0 | 32 | 33 | 0 |
| $p_T(W)$ Model | 3 | 3 | 3 | 7 | 7 | 7 |
| PDFs | 11 | 11 | 11 | 16 | 17 | 16 |
| QED radiation | 11 | 12 | 11 | 8 | 1 | 1 |
| M_W | - | - | - | 9 | 9 | 9 |
| Total Systematic | 39 | 27 | 26 | 78 | 70 | 23 |
| Statistical | 48 | 54 | 0 | 60 | 67 | 0 |
| Total | 62 | 60 | 26 | 98 | 97 | 23 |

Direct measurements of the W boson width have been obtained by CDF (using 350 pb⁻¹) and DØ (using 180 pb⁻¹ of data) from the fit to the transverse mass (m_T) spectrum of $W \rightarrow \ell\nu$ decays in the high m_T region, where the Γ_W Breit-Wigner lineshape dominates over the detector resolution Gaussian lineshape. The modeling of the m_T spectrum is done using the Monte Carlo (MC) simulation. The MC m_T templates are normalized to the data in the region of $50 < m_T < 100$ GeV/c², and the fit is performed in $100 < m_T < 200$ GeV/c² to extract Γ_W (see Fig. 1).

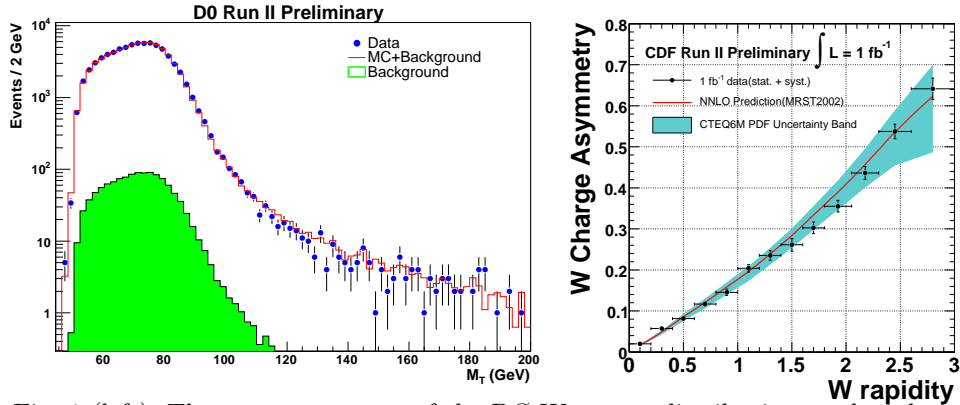


Fig. 1 (left). The transverse mass of the DØ W events distribution used to determine the W width. The fit is performed in the region of 100–200 GeV. (Right). CDF measured $A|_{y_W}$ compared to CTEQ6M prediction. The band illustrates the range of uncertainty on the CTEQ prediction.

The most precise measurement comes from CDF, which upon combining electron and muon channels gives $\Gamma_W = (2032 \pm 71) \text{ MeV}/c^2$, in good agreement with the SM prediction of $(2093 \pm 3) \text{ MeV}/c^2$ [7]. This is the world's most precise single measurement to date that reduces the world average uncertainty by 22%. Systematic uncertainties are of similar sources to M_W measurement and are summarized in Table 1.

2.2. W and Z boson production and asymmetries

Precise measurements of the rapidity distributions of W and Z can provide the constraints on the PDFs. In the W case, the constraints can be obtained by measuring the W charge asymmetry.

W Charge asymmetry. $W^+(W^-)$ bosons at the Tevatron are produced by annihilation of the valence $u\bar{d}(\bar{d}u)$ quarks. Since $u(\bar{u})$ quarks carry on the average a higher fraction of the $p(\bar{p})$ momentum than the $d(\bar{d})$ quarks, a $W^+(W^-)$ tends to be boosted in the direction of the $p(\bar{p})$ beam. This results in a W charge asymmetry $A(y_W)$, where y_W is the rapidity of the W boson. The production cross section distributions $d\sigma(W^\pm)/dy_W$ are sensitive to the difference between the u and d -quark PDFs and provide an important input to the global PDF fits. Since the longitudinal component of the neutrino momentum (p_z') is not known, a measurement of the lepton charge asymmetry $A(\eta_\ell)$ is traditionally made, where η_ℓ is the lepton pseudorapidity. Such a charge asymmetry in muons has been measured by DØ using 300 pb^{-1} of data [8].

Stronger constraints on PDFs can be placed by extracting y_W directly using a new analysis method, which was recently presented by CDF. The new technique constrains events to $M_W = 80.4 \text{ GeV}/c^2$. That results in two solutions for p_z' , where each solution receives the weight according to the $W \rightarrow \ell\nu$ angular decay structure and $\sigma(W^\pm)$. The procedure is iterated to eliminate a dependence of the weighting factor on the asymmetry itself. The method is applied to $W \rightarrow e\nu$ events using 1 fb^{-1} of CDF data. The measured W charge asymmetry as a function of $|y_W|$ is shown in Fig. 1 compared to the CTEQ5L PDF prediction. The experimental uncertainties are lower than the uncertainties from the PDFs. They will help to constrain the PDFs in future fits and in particular reduce the PDF uncertainty on future M_W and Γ_W measurements.

The measurement of the Z boson rapidity probes quarks with low proton and anti-proton momentum fractions x and high four-momentum transfer squared Q^2 ($Q^2 \approx M_Z^2$). It is a stringent test of QCD calculations. CDF analyzed e^+e^- pairs with pseudorapidities $|\eta_e|$ up to 2.8 near the M_Z peak region using 1.1 fb^{-1} of data. The result is consistent with NLO CTEQ6 PDF as shown in Fig. 2, and will be used as a future input to PDF fits.

A measurement of Z/γ^* transverse momentum (q_T) distribution was performed by DØ in e^+e^- events ($40 < M_{ee} < 200 \text{ GeV}/c^2$) using 1.0 fb^{-1} of data. At low q_T , the results (Fig. 2) are in agreement with the simulation from the ResBos event generator [9], which does a soft gluon resummation using the CSS technique [10], while at high q_T ($q_T \gtrsim 20 \text{ GeV}/c$), the cross section is dominated by radiation of a

single parton with a large transverse momentum, and the results are in agreement with the fixed-order perturbative QCD, now available at the NNLO [11].

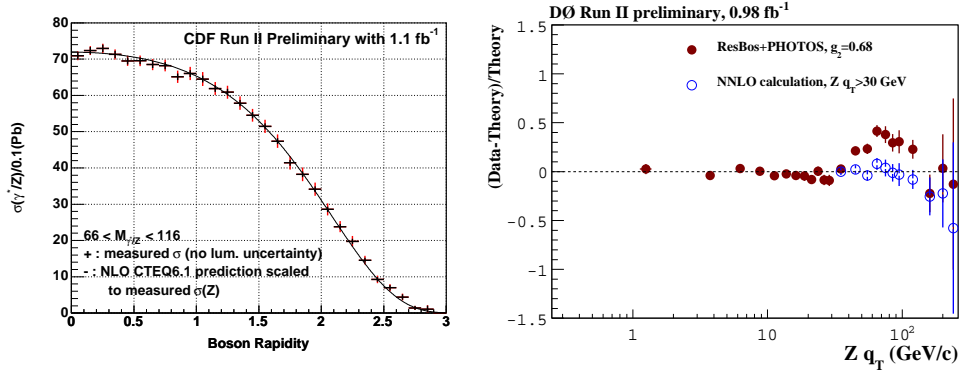


Fig. 2 (left). CDF measured $d\sigma(Z^0/\gamma^* \rightarrow e^+e^-)/dy$ distribution in the $66 < M_{ee} < 116 \text{ GeV}/c^2$ region compared to the calculation with NLO CTEQ6.1 PDFs. (Right). The fractional difference between $D\bar{O}$ measured differential cross section $d\sigma(Z^0/\gamma^* \rightarrow e^+e^-)/dq_T$ and the theoretical predictions.

2.3. Diboson production

An important test of the SM is the measurements of the diboson pair production cross-sections. Deviations from the rates predicted by the SM or in kinematics of observed events could point at anomalies in triple gauge boson couplings (TGCs), which are directly related to the non-Abelian $SU(2)_L \otimes U(1)_Y$ group structure, and could indicate new particles in loop diagrams [12]. Measurements at the Tevatron probe higher \sqrt{s} than are available at LEP and are sensitive to different combinations of TGCs. Diboson final states can also receive contributions from the s -channel production of an as yet unobserved particle, such as the SM Higgs decaying to a pair of W bosons.

Of the heavy diboson processes, WW production is the largest one. The highest statistics measurement of WW cross-section to date was performed by CDF using 825 pb⁻¹ dataset. The measured cross-section is $\sigma = 13.6 \pm 2.3(\text{stat}) \pm 1.6(\text{syst}) \pm 1.2(\text{lum})$ pb, in agreement with the NLO calculations of 12.4 ± 0.8 pb [13].

The WZ process has a smaller cross section and has been only recently observed at the Tevatron [14]. Since then both CDF and $D\bar{O}$ have updated the WZ cross-section measurements with larger datasets and set tight limits on TGCs. The largest dataset (1.9 fb⁻¹) of trilepton (e, μ) events has been analyzed by CDF. With 25 events observed in the WZ signal region, while expecting only $5.2 \pm 0.5(\text{stat}) \pm 0.6(\text{syst})$ background events, the significance of the excess is more than 6 standard deviations, and the measured WZ cross-section $\sigma = 4.3^{+1.3}_{-1.0}(\text{stat}) \pm 0.2(\text{syst}) \pm 0.3(\text{lum})$ pb stands in good agreement with an NLO prediction of 3.7 ± 0.1 pb [13].

ZZ process has one of the smallest cross sections at the Tevatron. The evidence of ZZ production with a significance of 3σ has been reported by CDF based on 1.5

fb⁻¹ of data. CDF analysis combines the 4 ℓ and 2 ℓ -2 ν final states, and measures $\sigma = 0.75_{-0.54}^{+0.71}$ pb consistent with the NLO calculation of 1.4 ± 0.1 pb.

$W\gamma$ production. The interference among the three tree-level diagrams involved in $W\gamma$ production creates a zero in the center-of-mass angular distribution θ^* , between the W and the direction of the upcoming quarks, corresponding to $\cos(\theta^*) = \pm\frac{1}{3}$. DØ measured the charge-signed rapidity photon-lepton difference in $W\gamma$ events sensitive to the radiation amplitude zero using 0.9 fb⁻¹ of data. The observed distribution is consistent with the SM prediction, as opposed to the alternative model with anomalous $WW\gamma$ couplings with no dipole moment and producing no dip in the expected region, as shown in Fig. 3.

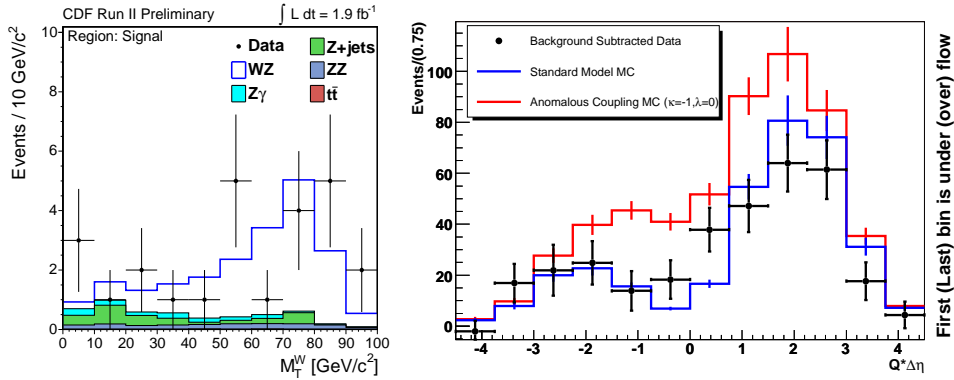


Fig. 3 (left). The transverse mass distribution of CDF WZ candidates in the WZ signal region. (Right). The DØ measured charge-signed rapidity $Q \times \Delta\eta$ difference shape as compared to the SM predictions and to a model with anomalous $WW\gamma$ couplings.

$Z\gamma$ production. In the SM at the tree level, a Z boson cannot couple to a photon, therefore an excess in $Z\gamma$ production would indicate anomalous $ZZ\gamma$ and $Z\gamma\gamma$ TGCs. CDF and DØ 1 fb⁻¹ samples of $\ell\ell\gamma$ events with photon transverse energy $E_T(\gamma) > 7$ GeV have been analyzed, and measured cross sections were found to be consistent with the SM predictions [15].

3. Top physics at the Tevatron

The top quark stands apart from other quarks in the SM due to its heavy mass of ≈ 175 GeV/ c^2 remarkably close to the electroweak scale and with the coupling to a Higgs boson close to unity. That makes some to speculate that the top may play a special role in the electroweak symmetry-breaking mechanism. In addition, this heavyweight object has a very short lifetime $\tau_t \sim 10^{-24}$ s and width $\Gamma \approx 1.5$ GeV, much larger than the scale for the perturbative QCD ($\Lambda_{QCD} \approx 200$ MeV). As a result it decays as a free quark, passing its momentum and spin directly to its decay products.

The top quark was discovered fairly recently by the CDF and DØ experi-

ments [16] during the Tevatron Run 1. With approximately 100 pb^{-1} of data collected by each experiment, event samples were statistically limited but sufficient to claim the discovery of the new quark. Now with over 20 times more data and even more data to come, the Tevatron experiments started achieving sensitivities for studying properties of the “unordinary” quark in great detail.

3.1. Top pair cross section measurements

The top quarks are produced at the Tevatron mainly in pairs strongly through the $q\bar{q}$ annihilation ($\sim 85\%$) or gluon-gluon fusion ($\sim 15\%$). Single top quarks can be produced via the electroweak interaction, which is discussed elsewhere [17].

In the SM, the top quark decays through charged-current weak interaction almost exclusively into a real W and a b quark. The final states of the top quark are classified by the W decays. The most sensitive channel for top quark mass measurements is the lepton+jets final state $t\bar{t} \rightarrow (\ell^- \bar{\nu}_b)(q_1 \bar{q}_2 b)$, where one W decays leptonically and the other one into a pair of quarks, representing about 30% of the $t\bar{t}$ decays. The signature is a single high- p_T lepton, missing E_T and four jets with dominant background from a W boson produced in conjunction with jets. The dilepton final state $t\bar{t} \rightarrow (\ell_1^+ \nu_1 b)(\ell_2^- \bar{\nu}_2 \bar{b})$ is the cleanest one, although it suffers from the smallest branching ratio of 5%. The all-hadronic final state $t\bar{t} \rightarrow (q_1 \bar{q}_2 b)(q_3 \bar{q}_4 \bar{b})$ has the highest branching ratio, but it is challenging due to swamping QCD backgrounds.

To reduce background contaminations, one employs algorithms to tag a b -quark jet from a top quark exploiting the long lifetime of the b -quark and reconstructing a displaced vertex with the silicon detectors. Other tagging algorithms are used to

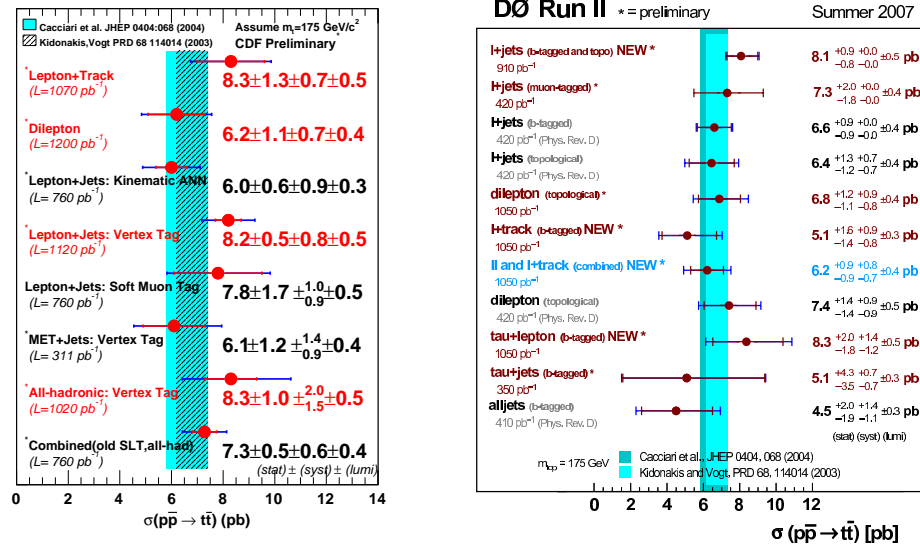


Fig. 4. Summary of the $t\bar{t}$ production cross section measurements performed by CDF (left) and D0 (right) experiments.

detect soft muons within a b -jet from the b -quark semi-leptonic decays, or discriminate a heavy flavor from light flavor jets on the statistical basis based on the track content within a jet.

Due to the top quark large mass, events with top quarks tend to be more energetic and central, and the $t\bar{t}$ events can be also separated from backgrounds without applying a b -tag requirement using kinematic and topological discriminators.

The $t\bar{t}$ cross section measurement is the first important step towards understanding of the top properties, and it has been measured by CDF and DØ in all of the $t\bar{t}$ decay channels using a variety of techniques. A summary of recent results from both experiments is presented in Fig. 4, all stand in agreement with the theoretical prediction of 6.7 ± 0.8 pb [18] at $m_t = 175$ GeV/ c^2 .

3.2. Top mass measurements

The top quark mass is a fundamental parameter of the SM, precise measurement of which together with the W mass constrains the Higgs mass. For this measurement a full reconstruction of the $t\bar{t}$ events is required, which presents several experimental challenges. The neutrinos from leptonically decaying W 's escape the detector. The quarks hadronize and form jets whose energy must be corrected back to the parton level. The assignment of jets to right partons usually has many possible permutations. Finally, there are background processes that can mimic $t\bar{t}$ events.

CDF and DØ performed measurements of the top mass in all of the top decay final states with a large diversity of sophisticated techniques. Current measurements achieved a level of precision when systematic uncertainties start to dominate. The main contribution to systematics comes from the knowledge of the jet energy scale (JES), which incorporates corrections of the raw jet energies and instrumental effects, and is known to a level of 2–3% [19]. A fairly recent important improvement to the top quark mass analyses is the *in situ* JES calibration technique, which introduces the JES as a second observable in the $t\bar{t}$ event reconstruction and makes use of distributions of the invariant di-jet mass m_W of the hadronically decaying W bosons. A simultaneous determination of m_t and the JES *in situ* effectively transforms the JES systematics into a statistical uncertainty, since with more statistics the knowledge of the shape of di-jet mass m_W distribution improves.

The summary of the top mass measurements is presented in Fig. 5. The most precise measurements from each channel using up to 1 fb^{-1} of the data were combined with Run 1 measurements, which results in the world average top quark mass of $170.9 \pm 1.1(\text{stat}) \pm 1.5(\text{syst}) \text{ GeV}/c^2$. The precision of this measurement supersedes the original projections made before Run 2, and at the end of Run 2 the top mass is expected to be known at the 1 GeV level.

Precise measurements of the top quark and W boson masses provide an important input to the global electroweak fit. Assuming the SM is the correct description of nature, the preferred value for the Higgs mass is $M_H = 76_{-24}^{+33} \text{ GeV}/c^2$, and the upper 95% confidence level (CL) limit is $144 \text{ GeV}/c^2$, without taking into account the LEP 2 direct limit [6].

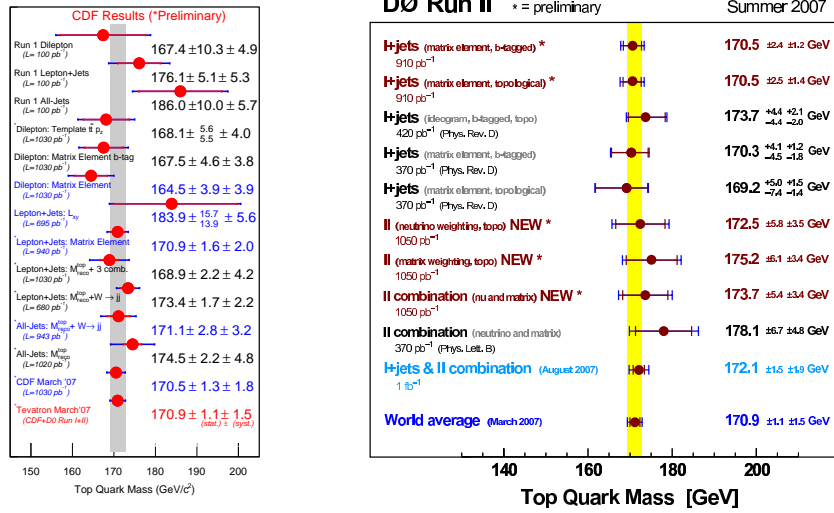


Fig. 5. Summary of the top quark mass measurements performed by CDF (left) and DØ (right) experiments.

3.3. Top quark properties

Forward-backward asymmetry in top pair production. Due to the large top quark mass, top production is an ideal testing ground to study effects predicted by QCD. NLO calculations predict a charge asymmetry in the $t\bar{t}$ production [20] arising from the interference of initial and final gluon radiation as well as from the interference of born and box diagrams. This charge asymmetry can be interpreted as the forward-backward asymmetry (A_{fb}) predicted at 4–6%. CDF measured the charged signed rapidity difference between top and anti-top quarks $\Delta y \cdot Q_\ell$, which is directly related to A_{fb} , using a 1.7 fb^{-1} sample of $\ell + \text{jets}$ events. The distribution of $\Delta y \cdot Q_\ell$ is shown in Fig. 6. The measured value $A = 0.28 \pm 0.13(\text{stat}) \pm 0.05(\text{syst})$ comes out higher than the NLO predictions, although consistent within errors.

Search for resonant top pair production. Resonant top production could arise from the decays of massive Z -like bosons in a topcolor-assisted technicolor [21] and several other theories beyond the SM (BSM) [22]. The CDF and DØ $\sim 1 \text{ fb}^{-1}$ samples of lepton + jets events were analyzed and no resonance peak has been observed in the $m_{t\bar{t}}$ spectrum (see Fig. 6). New improved limits on the mass of Z -like boson for various BSM scenarios have been set.

$\sigma(gg \rightarrow t\bar{t})/\sigma(p\bar{p} \rightarrow t\bar{t})$ measurement. The fraction of the $t\bar{t}$ events produced via gluon fusion is predicted with large uncertainties [18], therefore the measurement of $\sigma(gg \rightarrow t\bar{t})$ is an important test of the perturbative QCD. It can also reveal an unknown top production mechanism. CDF employs an observed correlation between the average number of gluons and the average number of low p_T charged particles, and extracts the $\sigma(gg \rightarrow t\bar{t})/\sigma(p\bar{p} \rightarrow t\bar{t})$ fraction by performing the fit (see Fig. 7) for the sample of the tagged $W + \geq 4$ events to gluon-rich (obtained from the

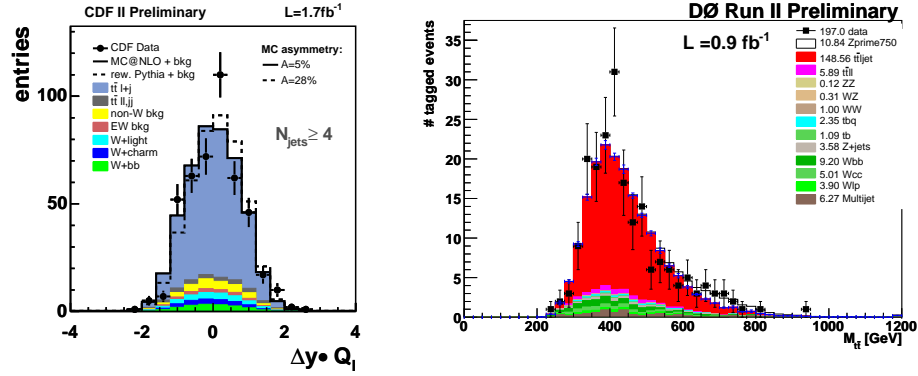


Fig. 6 (left). Reconstructed $\Delta y \cdot Q_\ell$ distribution. The dashed distribution correspond to predictions with $A=28\%$. (Right) Invariant $t\bar{t}$ mass spectrum.

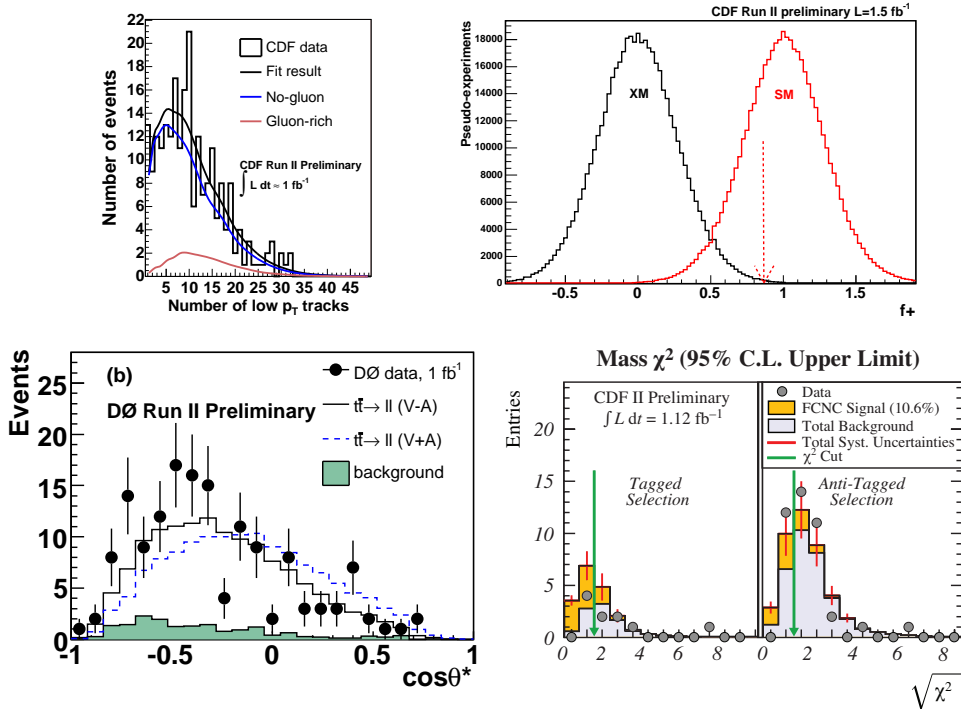


Fig. 7 (left top). The $\sigma(gg \rightarrow t\bar{t})/\sigma(p\bar{p} \rightarrow t\bar{t})$ fit result for CDF $W + 4$ or more jet sample. The two components of the fit gluon-rich and no-gluon are shown. (Left top) Probability distributions of the fraction of signal SM pairs f^+ and the outcome of the top quark charge measurement shown as an arrow. The data prefers the top quark charge of $\pm 2/3$ as expected from the SM. (Left bottom) $\cos\theta^*$ distribution of $D\bar{O}$ dilepton candidates. (Right bottom) The χ^2 distribution for both the tagged and anti-tagged CDF FCNC selections. The signal regions for the two selections are to the left of the green arrows.

di-jet sample) and no-gluon component (obtained from the $W + 0$ jet sample). The result of the measurement using 0.95 fb^{-1} of data is $0.07 \pm 0.14(\text{stat}) \pm 0.07(\text{syst})$, in agreement with the SM.

The other CDF analysis takes advantage of the kinematic shape differences between the $q\bar{q} \rightarrow t\bar{t}$, $gg \rightarrow t\bar{t}$ and backgrounds and by using the artificial neural network framework with 0.95 fb^{-1} of dataset obtains that the measured ratio is below 0.33 at 68% CL.

A direct measurement of top quark width is performed by CDF in a sample of the fully reconstructed $t\bar{t} \ell + \text{jets}$ events using 1 fb^{-1} of data by fitting the observed reconstructed top mass distribution to the top mass templates, corresponding to various top quark widths obtained from MC simulation. Applying the Feldman-Cousins prescription [23], CDF extracted a limit on the top width to be $\Gamma_t < 12.7 \text{ GeV}$ at 95% CL, assuming $m_t = 175 \text{ GeV}/c^2$.

Top charge. CDF performed a measurement of the top quark charge by discriminating two hypotheses: SM ($t \rightarrow W^+b$) vs. an exotic model ($Q \rightarrow W^-b$), suggesting a quark with the charge of $\pm 4/3$ [24]. The measurement is performed in both $\ell + \text{jets}$ and dilepton channels using 1.5 fb^{-1} of data. The charge of the $t(\bar{t})$ is obtained based on the pairing between the W boson and the b -jet determined with a high purity from the full reconstruction of the $t\bar{t}$ events, and based on a flavor tagging of the b -jet. The b -flavor tagging algorithm analyzes the track charges inside of the b -jet and assigns the b or \bar{b} probability with a purity of 61%. *A priori* defining the probability of incorrectly rejecting the SM to be 1%, the exotic quark hypothesis is excluded with 87% CL.

W helicity in top decays is fixed by the $V-A$ structure of the tWb vertex and it exhibits itself in the kinematics of the W decay products. SM predicts the fraction of decays to longitudinally polarized W bosons f_0 to be $\approx 70\%$, and the fraction of left-handed W 's f_- is $\approx 30\%$, while the right-handed fraction f_+ is suppressed. Both experiments measure the angular distribution of the charged leptons in the W rest frame with respect to the direction of the W boson motion in the top-quark rest frame ($\cos\theta^*$). Using 1 fb^{-1} of $\ell + \text{jets}$ and dilepton candidates, DØ measures $f_+ < 0.14$ at 95% CL (see Fig. 7). CDF performed two independent measurements using 1.7 fb^{-1} of data. The best limit is $f_+ < 0.07$ at 95% CL.

Search for FCNC $t \rightarrow Zq$ decays. In the SM, top quark flavor changing neutral current (FCNC) decays are highly suppressed with branching fractions of the order of 10^{-14} . In SUSY and two Higgs double models branching ratios are higher, up to 10^{-2} . CDF searched for the FCNC decays of top in $Z + \geq 4$ jet candidate events with and without a secondary vertex b -tag in 1.1 fb^{-1} of data, by reconstructing events under the $t\bar{t}$ FCNC decay hypothesis and quantifying the goodness of the fit with the χ^2 term. Distributions of χ^2 are shown in Fig. 7. CDF sets an upper limit $B(t \rightarrow Zq) < 10.6\%$ at 95% CL.

4. Conclusions

In this article recent CDF and DØ results in the electroweak and top sector are presented based on the datasets of up to 1.7 fb^{-1} . The electroweak measurements bring SM tests to a level of precision which meets or exceeds that of electron-positron colliders. Precision measurements of the mass of the W boson (0.04%) and the mass of the top quark (1.1%) place limits on the mass of the SM Higgs boson to be less than $144 \text{ GeV}/c^2$ at 95% CL. Many properties of the top quark have been analyzed in detail, while more precise measurements are expected with larger datasets. The Tevatron Run 2 is well underway and is projected to increase the statistics of datasets by a factor of four above those reported here.

References

- [1] D. Acosta et al. [CDF Collaboration], Phys. Rev. D **71** (2005) 032001; V. Abazov et al. [DØ Collaboration], Nucl. Inst. Meth. A **565** (2006) 463.
- [2] D. Acosta et al. [CDF Collaboration], Phys. Rev. Lett. **94** (2005) ; A. Abulencia et al. [CDF Collaboration], Phys. Rev. D **75** (2007) 092004; V. Abazov et al. [DØ Collaboration], Phys. Rev. D **71** (2007) 072004.
- [3] C. Anastasiou et al., Phys. Rev. D **69** (2004) 094008.
- [4] S. Klimenko, J. Konigsberg and T. Liss, FERMILAB-FN-0741 (2003); T. Edwards et al., FERMILAB-TM-2278-E (2004).
- [5] T. Aaltonen et al. [CDF Collaboration], arXiv:0707.0085v1.
- [6] The LEP Electroweak Working Group, <http://lepewwg.web.cern.ch/LEPEWWG/>
- [7] W. M. Yao et al., J. Phys. G **33** (2006) 1.
- [8] V. Abazov et al. [DØ Collaboration], arXiv:0709.4254v1.
- [9] C. Balazs and C. P. Yuan, Phys. Rev. D **56** (1997) 5558.
- [10] J. Collins, D. Soper and G. Sterman, Nucl. Phys. B **250** (1985) 199.
- [11] K. Melnikov and F. Petriello, Phys. Rev. D **74** (2006) 114017.
- [12] J. Ellison and J. Wudka, Ann. Rev. Nucl. Part. Sci. **48** (1998) 33.
- [13] J.M. Campbell and R.K. Ellis, Phys. Rev. D **60** (1999) 113006.
- [14] A. Abulencia et al. [CDF Collaboration], Phys. Rev. Lett. **98** (2007) 161801.
- [15] V. Abazov et al. [DØ Collaboration], Phys. Rev. B **653** (2007) 378.
- [16] F. Abe et al. [CDF Collaboration], Phys. Rev. Lett. **74** (1995) 2626; S. Abachi et al. [DØ Collaboration], Phys. Rev. Lett. **74** (1995) 2632.
- [17] J. Mitrevski, Fizika B (Zagreb) **17** (2008) 181.
- [18] M. Cacciari et al., J. High Energy Phys. **0404** (2004) 068; N. Kidonakis et al., Phys. Rev. D **68** (2003) 114014.
- [19] A. Bhatii et al. [CDF Collaboration], Nucl. Inst. Meth. A **566** (2006) 375; J. Kvita [DØ Collaboration], AIP Conf. Proc. 867 (2006) 43.
- [20] J.H. Kühn and G.Rodrigo, Phys. Rev. Lett. **81** (1998) 40, Phys. Rev. D **59** (1999) 054017.
- [21] C. Hill and S. Park, Phys. Rev. D **49** (1994) 4454.

- [22] A. Leike, Phys. Rep. **317** (1999) 143; J. Rosner, CERN-TH/96-169 (1996); T. Rizzo, Phys. Rev. D **61** (2000) 055005; L. Sehgal and M. Wanninger, Phys. Lett. B **200** (1988) 211.
- [23] G. Feldman and R. Cousins, Phys. Rev. D **57** (1998) 3873.
- [24] D. Chang, W. Chang and E. Ma, Phys. Rev. D **59** (1999) 091503.

t-KVARKOVSKI I ELEKTROSLABI REZULTATI NA TEVATRONU

Predstavljamo nove ishode CDF i DØ mjerenja o svojstvima W i Z bosona te t-kvarka.